Rock and Soil Mechanics

Volume 41 | Issue 3 Article 9

9-27-2020

Study on the mechanism of circumferential yielding support for soft rock tunnel with large deformation

Sheng-xiang LEI
China Railway Construction Corporation Limited, Beijing 100855, China

Wei ZHAO
Key laboratory Transportation Tunnel Engineering, Ministry of Education, Southwest Jiaotong University, Chengdu, Sichuan 610031, China, swjtu_zhao@126.com

Custom Citation

LEI Sheng-xiang, ZHAO Wei, . Study on the mechanism of circumferential yielding support for soft rock tunnel with large deformation[J]. Rock and Soil Mechanics, 2020, 41(3): 1039-1047.

Rock and Soil Mechanics 2020 41(3): 1039−1047 ISSN 1000−7598
https: //doi.org/10.16285/j.rsm.2019.5545 rocksoilmech.researchcommons.org/journal

Study on the mechanism of circumferential yielding support for soft rock tunnel with large deformation

LEI Sheng-xiang[1, 2, 3], ZHAO Wei[1, 2]

1. School of Civil Engineering, Southwest Jiaotong University, Chengdu, Sichuan 610031, China
2. Key laboratory Transportation Tunnel Engineering, Ministry of Education, Southwest Jiaotong University, Chengdu, Sichuan 610031, China
3. China Railway Construction Corporation Limited, Beijing 100855, China

Abstract: It is difficult for traditional bolt-shotcrete support to meet the requirements of deformation control in soft rock tunnel, therefore yielding support becomes an important means to control deformation. The circumferential yielding support sets up the yielding device in the circumferential direction of the tunnel in order to realize the rigid-flexible-rigid characteristics of the supporting structure. From the perspective of energy transformation in tunnel excavation-support process, the principle of circumferential yielding support is clarified in this paper. The main factors affecting the deformation of the support structure are analyzed using the analytical method of structural mechanics, and the mechanical characteristics of traditional support and circumferential yielding support are compared using the finite element software - ABAQUS. The following conclusions are drawn: (1) The initial support is a typical compression-bending member. The circumferential yielding support causes the yielding device to buckle through the circumferential pressure, which balances with the internal force of the support structure. It is hence possible to achieve a certain support resistance while controlling the surrounding rock stress by shortening the circumference. (2) The circumferential yielding device should be set at places where the bending stress is relatively small. The shear stiffness and bearing capacity of the device should be ensured with the characteristics of "strong shear and weak compression". (3) The circumferential yielding support has the mechanical characteristics of rigid-flexible-rigid, which can be adapted to the rheological characteristics of soft rock with high geo-stress.

Keywords: soft rock tunnel; large deformation; circumferential yielding support

1 Introduction

As China's strategic infrastructure construction advances to the complex and arduous mountainous areas in the west, such as the currently ongoing Sichuan–Tibet Railway and Yunnan–Tibet Railway, the large deformation of soft rocks has become one of the problems that brings difficulties to the construction of mountain tunnels, showing characteristics such as strong rheological properties, large tectonic stresses and squeezable deformations.

There have been many successful cases of controlling large deformation of soft-rock tunnels around the world, such as the Tauern Tunnel in Austria[1] and the Huina Mountain Tunnel in Japan[2] using long anchors and retractable supports, and Wushaoling Tunnel in China[3] adopting the method of two-layer primary support and two-layer lining support. However, from the perspective of engineering practice and research status, the support method for soft-rock tunnel is still not mature enough, and the control theory of large deformation of soft-rock tunnel should be further explored.

Germany began to use U-shaped steel retractable brackets in mines back to 1932[4], which was the early application of circumferential yielding supporting structure; Aydan et al.[5] summarized the squeezing deformation failure of the tunnel based on specific cases and proposed a method for predicting tunnel squeezing deformation failure based on tunnel depth and uniaxial compressive strength. Kovari et al.[6] pointed out that the brittleness of shotcrete was incompatible with the deformation of the surrounding rock, and proposed a "buckling control" support method that slotted at the connection of the steel arch ribs; Jiang et al.[7] theoretically studied the development law of loosening pressure and plastic zone of soft rock tunnels. The cavern stability was comprehensively considered based on the formation characteristic curve, and proposed a method to estimate the stability of surrounding rock by the relationship between the minimum support resistance and the strain of surrounding rock; Cantieri et al.[8] studied the interaction between yielding support and surrounding rock; He et al.[9] developed a constant resistance anchor rod suitable for large deformation of soft rock; Tian et al.[10] carried out numerical study on the installation of buckling elements in the circular cavity support structure; Wang et al.[11−12] discussed the characteristics and development trend of soft-rock tunnel support technology, and pointed out that yielding support

Received: 30 March 2019 Revised: 29 July 2019
This work was supported by the National Key R&D Program of China(2018YFC0808702，2018YFC0808706) and the Open Fund for Strengthening Engineering Materials and Structures in Key Laboratories of Universities in Fujian Province(B170001-1).
First author: LEI Sheng-xiang, male, born in 1965, PhD, Professorate senior engineer, doctoral supervisor, mainly engaged in the technical development and management of tunnel and underground engineering. E-mail: 18192088688@163.com
Corresponding author: ZHAO Wei, male, born in 1977, PhD candidate, Senior engineer, mainly engaged in the analytical work of tunnel and underground engineering. E-mail: swjtu_zhao@126.com

is the best measure to control large deformation of soft rock; Qiu et al.[13] developed an extreme energy dissipation supporting structure that adapts to large deformation of tunnel. The structure was applied to the deep-buried old loess section and high in-stress horizontal rock section of the Yangshan tunnel of the Menghua Railway.

The above research has achieved certain results in the development of tunnel yielding support but were more focused on the conceptual, qualitative analysis and experimental research. The mechanical response of the supporting structure is less explored. Further analysis is therefore required, from the perspective of structural mechanics, to understand the stiffness, internal force and yielding characteristics of the yielding supporting structure.

From the perspective of transformation of potential energy stored within the surrounding rock during the excavation-supporting process, this paper combines the mechanical analysis of the internal force and displacement of the circular tunnel supporting structure to analyse the mechanical principles of the circumferential yielding of the supporting structure. Moreover, the paper discusses the selection basis of installation location for the metal buckling-type yielding devices. Finally, the finite element software ABAQUS is used to study the applications of the circumferential yielding support.

2 Energy transformation of tunnel excavation and support

Tunnel excavation breaks the initial equilibrium state of surrounding rock, stress is redistributed, mechanical behaviours such as elastoplastic deformation of surrounding rock can display, which can be regarded as the result of the release of the original potential energy accumulated in rock mass.

Cook and Salamon considers the rock mass as a homogeneous linear elastic body, and gives the expressions of energy conservation:

$$W_{\mathrm{c}}+U_{\mathrm{m}}=U_{\mathrm{c}}+W_{\mathrm{r}} \tag{1}$$

where W_{c} is the work done by the internal stress of rock mass due to tunnel excavation; U_{m} is the strain energy released by the rock excavated by tunnelling; W_{r} is the strain energy re-accumulated within the rock body during the tunnel excavation; W_{r} is the loss of elastic energy during the cavern excavation.

Zhu[14] further studied the expression (1) of energy conversion during tunnel excavation and support.

$$W_{\mathrm{c}}+U_{\mathrm{m}}=U_{\mathrm{c}}'+W_{\mathrm{r}}+W_{\mathrm{n}}+W_{\mathrm{f}} \tag{2}$$

$$U_{\mathrm{c}}'+W_{\mathrm{n}}+W_{\mathrm{f}}\approx\text{constant} \tag{3}$$

where U_{c}' is the elastic energy re-accumulated within the surrounding rock; W_{n} is the inelastic strain energy lost in the surrounding rock; W_{f} is the energy absorbed by the supporting structure.

Equations (2) and (3) signify the energy transformation law during tunnel excavation and support. After the tunnel is excavated, the viscous, plastic, brittle fracture and local damage of the rock mass will dissipate and re-accumulate part of the energy as W_{n} and U_{c}', and the supporting structure will absorb part of the energy W_{f}. When the properties of the surrounding rock and the tunnel form are determined, W_{c}, U_{m} and W_{r} can be considered as almost unchanged. The above energy equations are basic principles that should be followed when analysing and controlling tunnel stability. Based on the understanding of the energy transformation of the surrounding rock, a reasonable construction system is designed, which can reduce U_{c}' by properly increasing W_{n} and W_{f}, so that the stability of the surrounding rock can be maintained. However, W_{n} is an inelastic energy loss, and excessive deformation of the surrounding rock will lead to high loose pressure, so W_{n} should be limited. Therefore, the reduction of U_{c}' should be achieved mainly by raising W_{f}, and this is realised in circumferential yielding support by setting the yielding devices.

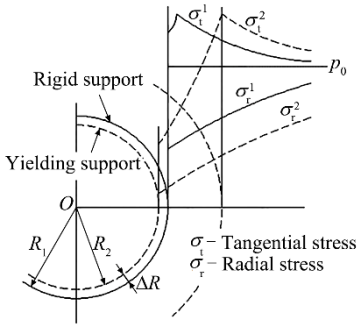

Fig.1 Principle of yielding support

Figure 1 is a schematic diagram illustrating the principle of the yielding support. It is assumed that the radius of the tunnel after rigid support is R_1 and after flexible support is R_2. The difference between the two is ΔR. The solid line indicates the situation of rigid support with almost no structural deformation, while the dashed line indicates the situation that the moderate deformation is allowed, σ_{r}^2 and σ_{t}^2 are smaller than that of rigid support. It can be seen from the figure that the tangential stress σ_{t} exceeds the original rock stress p_0, resulting in a compacted area inside the surrounding rock, which improves the bearing capacity of the surrounding rock. The compaction effect of σ_{t} is an important reason why the surrounding rock re-accumulates strain energy U_{c}' during excavation. However, it is not the higher of σ_{t} the better, this is because that if the total

effective stress of the surrounding rock exceeds the ultimate bearing capacity, it will cause the surrounding rock to be instable. The supporting structure and surrounding rock have a certain amount of deformation in the radial direction, which enlarges the range of the plastic zone. Lowering σ_t means the decrease of U_c', which is consistent with the energy supporting theory. Therefore, the yielding support not only reduces the tangential stress in the surrounding rock but also reduces the pressure of the surrounding rock, which protects both the surrounding rock and the supporting structure by yielding.

The pressure of the surrounding rock does work on the supporting structure, and the energy transformed into the supporting structure can be divided into

$$W_f = W_e + W_P \tag{4}$$

where W_e is the elastic energy stored in the support; W_P is the energy consumed by plastic deformation of the support.

Figure 2(a) is the traditional support structure, which stores and consumes energy through elastic-plastic deformation of the support itself ($W_e + W_P$) and the amount of energy transformed is low. Figure 2(b) is the support structure installed with the buckling-type circumferential yielding device that innovates on the methods of storing and consuming energy through the elastic deformation and plastic deformation of the support structure, respectively. Drawing on the energy dissipation principle of metal buckling, using the yielding device made of Q235 steel with high-ductility, W_f is increased by applying work on the yielding device through the circumferential pressure (axial force) of the support structure as well as the pressure of the surrounding rock does work in the radial direction of the tunnel. In the process of yielding, the main component of the supporting structure is kept in a working state below its ultimate strength, so that the ability of the supporting structure to resist deformation increases with the increase of the deformation of the surrounding rock, which is the primary condition for surrounding rock and supporting structure to reach stability. From the perspective of stress redistribution of the surrounding rock, yielding further adjusts the stress in order to form a self-balanced, circumferential bearing environment of the surrounding rock.

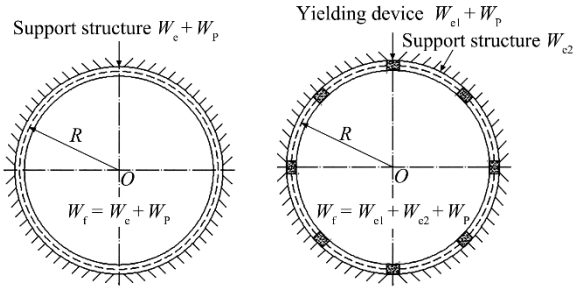

(a) Traditional support structure (b) Circumferential yielding support structure

Fig.2 Schematic diagrams of support structure

3 Mechanical analysis of internal force and convergence value of supporting structure

Studying the internal forces of the supporting structure and the influencing factors of its deformation is the prerequisite for the scientific development of yielding support. Although tunnels have various forms and mechanical analysis is difficult, such analysis of the special cross-section of supporting structure in combination with mathematical expressions of the relevant influencing factors are going to help understand the basic principles of the yielding support. Therefore, mechanical analysis is an important means to study yielding support. The paper studies the initial support of a circular tunnel with unit length taken along the tunnel axis as shown in Fig. 3. The radius of the initial support is assumed to be *R*, the vertical pressure is *q*, and the ratio of horizontal pressure to vertical pressure is λ. A symmetrical structure has an antisymmetric internal force of 0 under a symmetrical load. According to this characteristic, 1/4 structure is taken as the calculation model. The force method is used to calculate the structure internal force while the radial convergence value of the structure is calculated using the unit load method.

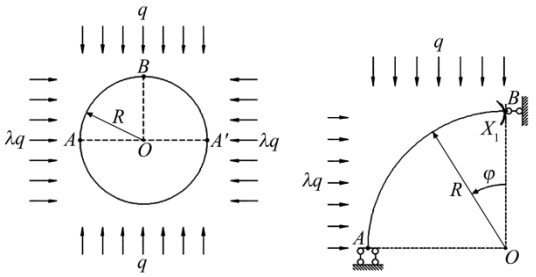

(a) Diagram of loading (b) Calculation diagram of basic structure

Fig.3 Calculation diagrams of circular support structure

3.1 Internal force calculation of supporting structure

Figure 3(b) is a statically indeterminate structure. The bending moment X_1 at point *B* is the unknown force. It is assumed that the axial force is positive if the axis is under compression and the bending moment is positive if the inner side of the axis is under tension. According to the condition that the rotation angle of point *B* is 0, a typical equation of the force method is established:

$$\delta_{11}X_1 + \Delta_{1q} + \Delta_{1(\lambda q)} = 0 \tag{5}$$

where δ_{11} is the intersection angle of the basic structure at point *B* when $X_1 = 1$, Δ_{1q} is the intersection angle of the basic structure at point *B* under the vertical pressure of *q*; $\Delta_{1(\lambda q)}$ is the intersection angle of the basic structure at point *B* under the horizontal pressure of λq.

The internal force of the basic structure under the unit

unknown excess force are: $\bar{M}_1=1$, $\bar{Q}_1=0$, $\bar{N}_1=0$. Calculate the coefficient and free term of formula (5) using the unit load method:

$$\left.\begin{aligned}
&\delta_{11}=\int\frac{\bar{M}_1^2}{EI}\mathrm{d}s=\frac{\pi R}{2EI}\\
&\Delta_{1q}=\int\frac{\bar{M}_1M_q}{EI}\mathrm{d}s=-\frac{1}{EI}\int_0^{\frac{\pi}{2}}\frac{q(R\sin\varphi)^2}{2}R\mathrm{d}\varphi=-\frac{\pi qR^3}{8EI}\\
&\Delta_{1(\lambda q)}=\int\frac{\bar{M}_1M_{\lambda q}}{EI}\mathrm{d}s=\frac{1}{EI}\int_0^{\frac{\pi}{2}}[\lambda qR^2(1-\cos\varphi)-\\
&\qquad\frac{1}{2}\lambda qR^2(1-\cos\varphi)^2]R\mathrm{d}\varphi=\frac{\pi\lambda qR^3}{8EI}
\end{aligned}\right\}\tag{6}$$

where EI is the bending stiffness; M_q is the bending moment of the basic structure under vertical pressure q; $M_{\lambda q}$ is the bending moment of the basic structure under horizontal pressure λq; s is the arc length of the basic structure; φ is the central angle corresponding to the arc length being integrated.

Substitute equation (5) to get the bending moment at point B:

$$X_1=\frac{1}{4}qR^2(1-\lambda)\tag{7}$$

According to the superposition principle, the bending moment expression of any cross section of the structure is obtained:

$$\begin{aligned}
&M_{q+\lambda q}=\bar{M}_1X_1+M_q+M_{\lambda q}=\frac{1}{4}qR^2(1-\lambda)-\\
&\frac{q(R\sin\varphi)^2}{2}+\lambda qR^2\left[(1-\cos\varphi)-\frac{1}{2}(1-\cos\varphi)^2\right]=\\
&\frac{1}{4}qR^2(1-\lambda)\cos2\varphi
\end{aligned}\tag{8}$$

By the cross-section method (see Fig.4), the horizontal and vertical equilibrium equations are established:

$$\left.\begin{aligned}
&\sum X=0,\ Q\sin\varphi+N\cos\varphi-\lambda qR\cos\varphi=0\\
&\sum Y=0,\ -Q\cos\varphi+N\sin\varphi-qR\sin\varphi=0
\end{aligned}\right\}\tag{9}$$

where Q is the section shear force; N is the section axial force.

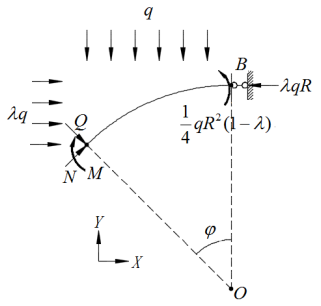

Fig.4 Calculation diagram of section method

Obtaining: $Q=\frac{1}{2}qR(\lambda-1)\sin2\varphi$,

$N=qR(\lambda\cos^2\varphi+\sin^2\varphi)$.

In summary, when loaded as shown in Fig.3, the internal force of the cross section of the circular supporting structure is

$$\left.\begin{aligned}
&M_{q+\lambda q}=\frac{1}{4}qR^2(1-\lambda)\cos2\varphi\\
&N_{q+\lambda q}=qR(\lambda\cos^2\varphi+\sin^2\varphi)\qquad\left(0\leqslant\varphi\leqslant\frac{\pi}{2}\right)\\
&Q_{q+\lambda q}=\frac{1}{2}qR(\lambda-1)\sin2\varphi
\end{aligned}\right\}\tag{10}$$

From equation (10), we can see that when $\lambda=1$, the bending moment M and shear force Q of the supporting structure are both 0, and when the circumferential axial force is $N=qR$, the structural stress is the same as the hydrostatic pressure.

When $\lambda\neq1$, the bending moment is 0 at $\varphi=\pi/4$, and the shear force reaches the extreme value. When $\varphi=0$ and $\varphi=\pi/2$, the bending moment reaches the extreme value.

3.2 Calculating convergence value of supporting structure

The radial convergence of the structure is represented by the relative displacement of A and A'. The calculation is based on the unit load method with the simplified calculation diagram in the virtual state shown in Fig.5.

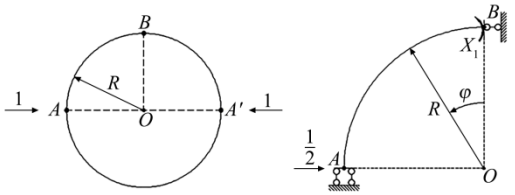

(a) Diagram of unit loading (b) Calculation diagram of unit load

Fig.5 Calculation diagram of unit load

The internal force of the structure under unit load is calculated using the force method:

$$\left.\begin{aligned}
&\bar{M}=R\left(\frac{1}{\pi}-\frac{\cos\varphi}{2}\right)\\
&\bar{N}=\frac{1}{2}\cos\varphi\\
&\bar{Q}=\frac{1}{2}\sin\varphi
\end{aligned}\right\}\tag{11}$$

According to the superposition principle, the radial displacement of a certain point on the structure can be obtained from superimposing the small displacement caused by each micro-segment deformation at that point:

$$\Delta=\int\frac{M_{q+\lambda q}\bar{M}}{EI}\mathrm{d}s+\int\frac{N_{q+\lambda q}\bar{N}}{EA_c}\mathrm{d}s+\int\frac{kQ_{q+\lambda q}\bar{Q}}{GA_c}\mathrm{d}s\tag{12}$$

where E is the elastic modulus; G is the shear modulus; A_c is the cross-sectional area of the supporting structure; EI is the bending stiffness; EA_c is the compressive stiffness; GA_c is the shear stiffness; k is the cross-sectional shear strain coefficient.

Substituting the internal forces obtained from equations (10) and (11) into equation (12) gives:

$$\Delta = \frac{(\lambda-1)qR^4}{24EI} + \frac{(2\lambda+1)qR^2}{6EA_c} + \frac{k(\lambda-1)qR^2}{6GA_c} \tag{13}$$

Since the mechanical analysis only considers 1/4 structure, the relative displacement of A and A' is

$$\Delta_{AA'} = 4\Delta = \frac{(1-\lambda)qR^4}{6EI} + \frac{2(2\lambda+1)qR^2}{3EA_c} + \frac{2k(\lambda-1)qR^2}{3GA_c} \tag{14}$$

Equation (14) is the analytical solution of the relative convergence value of A and A''. When the cross section is rectangular, k = 1.2. The three terms on the right side of the equation respectively represent the contribution of the structural bending deformation, axial deformation, and shear deformation to the radial convergence value. When the load mode and structural form are determined, the displacement will depend on the flexural stiffness (EI), compressive stiffness (EA_c) and shear stiffness (GA_c) of the section.

Assume that the supporting structure is C35 shotcrete with a thickness of 0.25 m. The calculation unit is taken as 1 m along the tunnel. Substituting the values of R = 3 m, E = 31.5 GPa, G = 13.125 GPa, and k = 1.2 into (13) gives:

$$\Delta = \Delta_M + \Delta_N + \Delta_Q = (16.483\,5 + 0.647\,6 + 0.109\,5)\times10^{-9}q = 17.240\,6\times10^{-9}q(\mathrm{m}) \tag{15}$$

where Δ_M , Δ_N and Δ_Q are the convergence values resulted from the bending moment, axial force and shear force, respectively. among them, $\Delta_M / \Delta = 95.609\%$; $\Delta_N / \Delta = 3.756\%$; $\Delta_Q / \Delta = 0.635\%$.

When q = 200 kN/m (equivalent to surrounding rock pressure of 0.2 MPa), Δ = 3.448 × 10^{-3} m, the convergence value of point A in Fig.3(a) is 2 Δ = 6.896 × 10^{-3} m

The above mechanical analysis shows that the convergence of traditional anchor-shotcrete support is dominated by bending deformation. It can be deduced the large deformation of the traditional supporting structure must be large bending deformation. With regard to the supporting material, the tensile strength of the shotcrete is much lower than its compressive strength, and thus having low resistance to the bending deformation, which essentially results in its structural failure. In addition, bending deformation and shear deformation change the shape of the supporting structure, which generates additional eccentric bending moments under the action of circumferential pressure. Therefore, for deeply-buried soft-rock tunnels, it is recommended to avoid improving the deformability of the supporting structure by reducing EI and GA_c .

Circumferential yielding support effectively leverages the high compressive strength of sprayed concrete. The circumferential yielding device should be designed based on the principle of reducing compressive rigidity, and the devices should be located at where small bending moment (or bending deformation) is observed in order to reduce the adverse effects of bending stress in the yielding area. At locations of small bending moment, the shear force is often large. To avoid shear dislocation caused by shear deformation, the yielding device should have enough shear stiffness and resistance. In other words, the device should be mechanically characterised with strong shear and weak compression.

It can be drawn from equation (10) that at $\varphi = \pi/4$, M = 0 is the minimum value. Despite that the circumferential pressure N at this location is not the maximum value, a proper mechanical design can allow the yielding device to play its role before the main supporting structure reaches its ultimate stress. Therefore, for the circular support structure, when the lateral pressure coefficient is $\lambda \neq 1$, the circumferential pressure yielding device should be set at the position of $\pi/4$, $3\pi/4$, $5\pi/4$, $7\pi/4$. According to formula (10), the characteristics of the supporting structure's internal force at this position are

$$M = 0\ ,\quad N = \frac{1}{2}qR(\lambda+1)\ ,\quad Q = \frac{1}{2}qR(\lambda-1) \tag{16}$$

4 Numerical analysis of metal buckling-type circumferential yielding support

4.1 Energy absorption mechanism of structural energy dissipation device

When loaded, the traditional supporting structures only allow small amount of elastic deformation[15], the elastic potential energy is stored to ensure the safety of the structure mainly by adjusting the performance (strength, stiffness, ductility) of the structure itself.

Energy dissipation technology is to set up energy dissipation devices in certain parts of the structure, and use them to generate friction, elastoplastic (or viscous, viscoelastic) deformation so that energy of the input structure is dissipated or absorbed in order to reduce the reaction of the main structure. The collapsible U-shaped steel supports commonly used in mine roadways are friction-type energy dissipation, and metal buckling-type circumferential yielding supports are elastoplastic energy dissipation.

Figure 6 is the stress-strain curve of the metal. The area of $ABCE$ represents the input work. The area of DCE represents the elastic energy stored in the metal at point C, and it is also the elastic energy released during unloading. The area of $ABCD$ represents the energy consumed by the plastic deformation of the metal, and which is mainly converted into thermal energy by the

friction of the internal lattice.

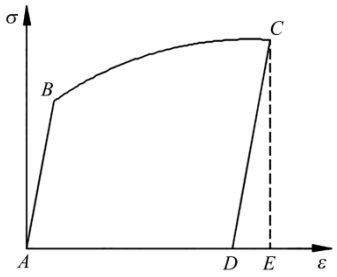

Fig.6 Stress–strain curves of metal

Q235 steel has the characteristics of low yielding point, excellent ductility, strong adaptability to environment and temperature, and low cost, which results in its wide utilization in the field of structural energy dissipation. Q235-grade steel is an ideal material for constructing metal buckling-type yielding instruments, and thus it is chosen to build the circumferential yielding device.

4.2 Numerical analysis of metal buckling-type yielding devices

As shown in Fig.7, the tunnel circumferential yielding device adopts two sets of annular structures composed of ϕ203 × 12 mm semi-circular steel pipes and flat plates with a thickness of 0.012 m. Two sets of diagonal bracing plates form a X-shaped built-in space; each set is consisted of 6 plates with a thickness of 0.01 m; the width of the middle plate is 0.08 m, and the width of the plates on both sides is 0.04 m. The thickness of the pressure device is slightly smaller than the thickness of the supporting structure (in this case, 0.2 m). Connection plates with a thickness of 0.012 m are set up on the top and bottom of yielding device with length of 1.0 m and width of 0.2 m. The ideal elastoplastic constitutive relation is assumed for Q235B steel with the elastic modulus E_s=206 GPa, yield strength f_y = 235 MPa, and ultimate strain ε_u = 0.04.

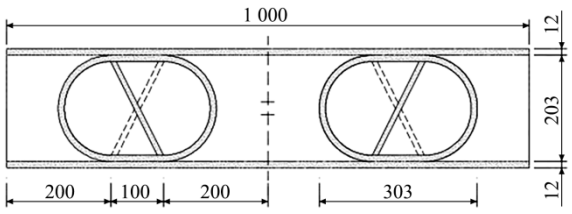

Fig.7 Metal buckling-type yielding device (unit:mm)

When the lateral pressure coefficient λ = 1.2, it is known from formula (10) that N = 11Q at the $\pi/4$ cross-section. ABAQUS is used to analyse the relationship between the shear pressure (N + Q) and the compression amount (U) of the yielding device. The international system of units (SI) is adopted; the unit of length is m, the unit of mass is kg, and the unit of force is N. C3D8R is chosen as the grid cell type and equivalent load mode selected with the single-stage loading N = 82.5 kN (equivalent to q = 25 kN/m in Fig.3) and Q = 7.5 kN. Load is applied through the coupling of the top plate and loading point with the bottom plate constraining all degrees of freedom. All parts are in hard contact.

Figure 8 shows the relationship between load and compression of the yielding device. The compression U is taken as the vertical displacement of the node in the middle of the top plate. The yielding device displays the characteristics of rigid-flexible-rigid due to buckling. When it is loaded to level 7.5, it begins to show flexible characteristics. At the time, the load N = 618.75 kN, Q = 56.25 kN. The compression of the yielding device tends to be stabilised towards level 15. While compression reaches 0.1035 m, the yielding is basically completed. At the time, the corresponding loads N = 1237.50 kN and Q = 112.50 kN. In the main yielding stage, the load–compression curve is having an approximately rectangular shape, showing obvious energy dissipation characteristics. After that, the support structure enters the rigid support stage, and further measures should be taken to enhance the support structure and improve the shear stiffness and bearing capacity of the yielding device to avoid shearing damage. The ultimate load allowance of the yielding device is up to level 30 corresponding to load N = 2475.00 kN, Q = 225.00 kN, and compression of 0.125 m.

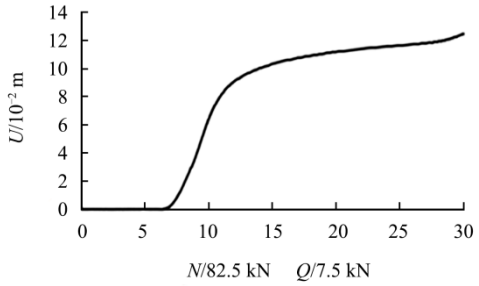

Fig.8 Load–compression curve of yielding device

Figure 9 shows the local Mises stress nephograms when the yielding device is loaded to level 15 and level 30, respectively. The X-shaped steel plates firstly undergo plastic deformation to absorb energy. The yield stress of the annular part is not yet to be reached when it is loaded to level 15, which improves the stability of the yielding structure (along the shearing direction of the supporting structure) during the subsequent loading process. When loaded to level 30, the annular part has not fully entered the plastic zone, which guarantees its shear resistance.

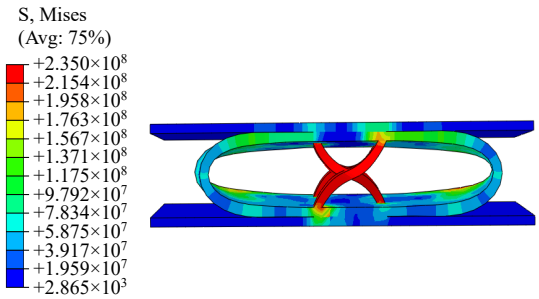

(a) Loaded to level 15

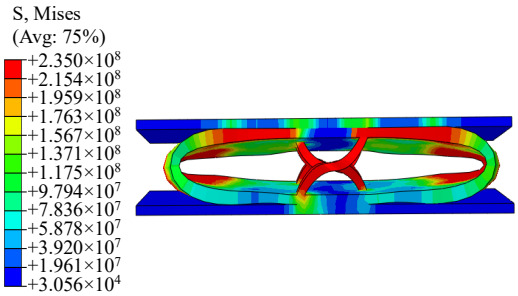

(b) Loaded to level 30

Fig.9 Mises stress nephogram of yielding device(unit: Pa)

4.3 Contrast analysis of yielding support structure and ordinary support structure

The study focuses on the calculation model shown in Fig.3. It is assumed that the supporting structure has a central radius, R is 3 m, λ is 1.2. The yielding devices are set along the circumferential direction at $\pi/4$, $3\pi/4$, $5\pi/4$, $7\pi/4$

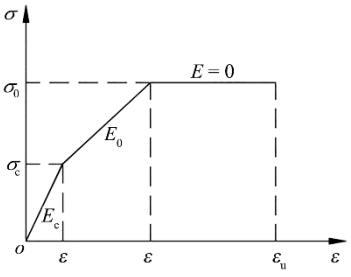

Fig.10 Stress–strain relationship of concrete

The supporting material is C35 shotcrete (the steel fibres reinforcement is not considered) with a thickness of 0.25 m and Poisson's ratio γ = 0.2. In accordance with China's concrete specifications, the constitutive relation of concrete materials is simplified to sectional linearity, as shown in Fig.10. The standard concrete ultimate compressive strength, σ_0 is 23.4 MPa; elastic ultimate strength, σ_c is 9.36 MPa; concrete elastic modulus, E_c is 31.5 GPa; concrete ultimate compressive strain, ε_u is 0.0033; and corresponding compressive strain, ε_0 is 0.002 when concrete stress reaches σ_c.

The finite element program ABAQUS is used to establish the quarter model of the supporting structure. The model established has the longitudinal length of the tunnel to be 1 m while B constrains U1 and UR3, A constrains U2 and UR3, and an arbitrary side constrain U3. C3D8R is chosen to be the grid cell type, and numerical analysis is performed considering situations when yielding devices are implemented and when they are not applied. Moreover, C3D8R is also chosen to be the grid cell type for the yielding device with all components in hard contact. The yielding device is connected with the supporting structure through binding constraints. The equivalent load mode is selected with single-stage loading q = 0.01 MPa, λq = 0.012 MPa (equivalent to q = 10 kN/m in Fig.3), the loading continues until any tiny area of the supporting structure reaches the ultimate strength σ_0 = 23.4 MPa.

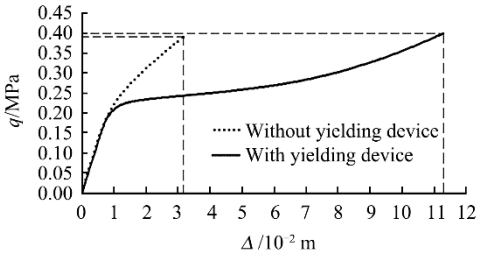

Fig.11 Characteristic curves of support structure

Figure 11 shows the characteristic curves of a supporting structure provided with and without yielding device, respectively. Δ is the convergence value corresponding to point A in Fig.3(b). Before the load q reaches 0.2 MPa, the supporting structures with and without yielding device demonstrate similar stiffness and provide similar resistance to the surrounding rock. As the load increases, the support stiffness of the two present obvious differentiation. For the support structure without any yielding devices, the limit convergence value at point A is only 3.17 × 10^{-2} m with the corresponding load q = 0.39 MPa, while the limit convergence value at point A of the supporting structure with the yielding device is 11.04 × 10^{-2} m with the corresponding load q = 0.4 MPa. The ultimate bearing capacity of the supporting structure (loaded until any tiny area of the supporting structure reaches the ultimate strength) is similar in both cases. The radial convergence value of the supporting structure equipped with yielding device is increased by 3.5 times, showing good flexibility. The convergence value at point A is assumed to be controlled to 8 × 10^{-2} m corresponding to load q = 0.302 3 MPa and 17.19 MPa for the maximum Mises stress of the supporting structure. The circumferential pressure N is used to shorten the circumference of the supporting structure, and the radial convergence of the supporting structure is mainly based on rigid

body displacement. At this stage, the shotcrete support structure is in a working state below the ultimate strength.

Figure 12 shows the Mises stress nephogram when the supporting structure is under the ultimate load. Figure 12(a) illustrates the traditional supporting structure. The bending deformation allows a very limited amount of yielding so that it is assumed to be a non-yielding supporting structure. Figure 12(b) shows the circumferential yielding support system (with the yielding device). Fig.12(c) is the circumferential yielding support structure (without the yielding device). Regardless of whether the yielding device is installed, the maximum stress appears at the inner side of the support structure *B* (see Fig.3(b)). Under the load of q = 0.4 MPa, the X-shaped built-in steel plates of the yielding device presents completely plastic buckling, while the circumferential structure only partially enters the plastic deformation state.

Since large shear force is exerted on the area where yielding device is installed, dislocation shear failure may be caused when the shear stiffness and bearing capacity are insufficient. The relative displacement ($U_D - U_C$) of the midpoints on the top and bottom plates of the yielding device (points *C* and *D* in Fig.12(d)) is taken as the reference index for shearing displacement.

Figure 13 shows the shear dislocation of the yielding device. When the limit load q = 0.4 MPa, the shear dislocation is 2.95×10^{-2} m. If the radial convergence of *A* (see Fig.3(b)) is targeted to be 8×10^{-2} m during the yielding stage, then the shear displacement is 1.81×10^{-2} m. This indicates that the metal buckling-type yielding structure provides a certain amount of shear rigidity with the ductility of Q235B steel avoiding shear brittle fracture.

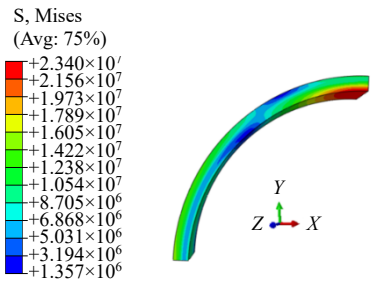

(a) Support structure without yielding（q = 0.39 MPa）

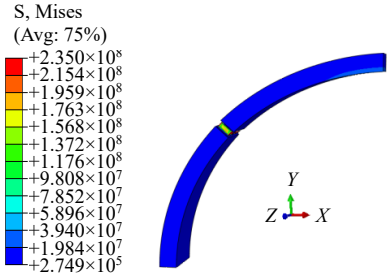

(b) Yielding support system（q = 0.40 MPa）

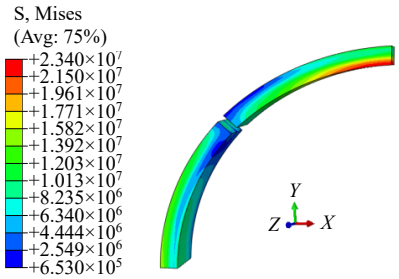

(c) Yielding support structure（q = 0.40 MPa）

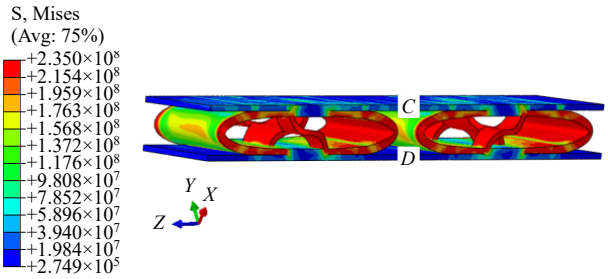

(d) Yielding device（q = 0.40 MPa）

Fig.12 Stress nephograms of support structure in ultimate limit state(unit: Pa)

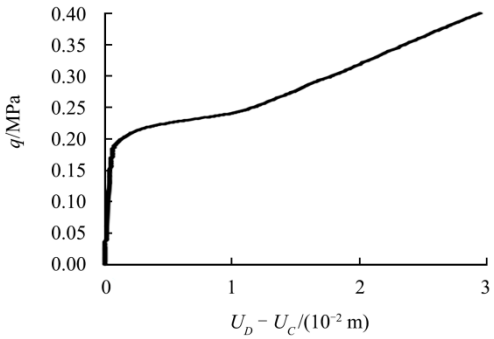

Fig.13 Shear dislocation of yielding device

The circumferential yielding support stores and dissipates energy through elastoplastic deformation so as to control the yielding amount. When the targeted yielding is achieved, the support system enters the “rigid” support stage that requires further measures to enhance the shear resistance of the yielding device. One of the measures is to connect the top and bottom plates of the yielding device through welding steel plates to the side. Moreover, improving the mechanical performance of supporting structure is the key to realise “post-rigidity”. Improvements can be achieved by implementing prestressed bolts (cables) post-yielding to adjust the internal force and stiffness of the structure, and to apply yielding bolts (cables) in the beginning of yielding to work together with the circumferential yielding support.

5 Conclusions

The preliminary support of soft-rock tunnels is attributed with compression-flexural property. When a large deformation

occurs, the support structure exhibits large bending deformation in combination with the additional bending moments contributed by the geometric nonlinearity. Shotcrete has low resistance to bending deformation, which is the main reason leading to the failure of the support structure.

The yielding support structure buckles the yielding device through circumferential pressure, which is in line with the characteristics of support system's internal force that help realize certain supporting resistance while adjusting stress and pressure of surrounding rock by shortening the circumference of the yielding device.

The yielding device should be set at where the bending moment is small. Meanwhile, areas with small bending moment are often experiencing large shear force. Therefore, it is important to make sure that the yielding device has sufficient shear stiffness and bearing capacity. In other words, the device should have the mechanical properties of "strong shear and weak compression".

References

[1] PETERSON R W, DUTTON P L, WAND A J. First and second tube of the Tauern Tunnel[J]. Geomechanik Und Tunnelbau, 2010, 3(4): 334–343.

[2] KIMURA F, OKABAYASHI N, KAWAMOTO T. Tunnelling through squeezing rock in two large fault zones of the Enasan Tunnel II[J]. Rock Mechanics & Rock Engineering, 1987, 20(3): 151–166.

[3] LI Guo-liang, ZHU Yong-quan. Control technology for large deformation of high land stressed weak rock in Wushaoling tunnel[J]. Jouranl of Railway Engineering Society, 2008(3): 54–59.

[4] LU Jia-liang. Support technology of soft rock roadway[M]. Changchun: Jilin Science and Technology Publishing House, 1995: 104–121.

[5] AYDAN Ö, AKAGI T, KAWAMOTO T. The squeezing potential of rock around tunnels: Theory and prediction with examples taken from Japan[J]. Rock Mechanics & Rock Engineering, 1996, 29(3): 125–143.

[6] KOVÁRI K, STAUS J. Basic considerations on tunnelling in squeezing ground[J]. Rock Mechanics & Rock Engineering, 1996, 29(4): 203–210.

[7] JIANG Y, YONEDA H, TANABASHI Y. Theoretical estimation of loosening pressure on tunnels in soft rocks[J]. Tunnelling & Underground Space Technology Incorporating Trenchless Technology Research, 2001, 16(2): 99–105.

[8] CANTIENI L, ANAGNOSTOU G. The interaction between yielding supports and squeezing ground[J]. Tunnelling & Underground Space Technology Incorporating Trenchless Technology Research, 2009, 24(3): 309–322.

[9] HE Man-chao, GUO Zhi-biao. Mechanical property and engineering application of anchor bolt with constant resistance and large deformation[J]. Chinese Journal of Rock Mechanics and Engineering, 2014, 33(7): 1297–1308.

[10] TIAN H M, CHEN W Z, TAN X J, et al. Numerical investigation of the influence of the yield stress of the yielding element on the behaviour of the shotcrete liner for yielding support[J]. Tunnelling & Underground Space Technology, 2018, 73: 179–186.

[11] WANG Bo, GUO Xin-xin, HE Chuan, et al. Analysis on the characteristics and development trends of the support technology of high ground stress tunnels in China[J]. Modern Tunnelling Technology, 2018, 55(5): 1–10.

[12] WANG Bo, WANG Jie, WU De-xing, et al. Study on application of yielding supporting system for large-deformation in soft rock Highway tunnel[J]. Journal of Railway Science and Engineering, 2016, 13(10): 1985–1993.

[13] QIU Wen-ge, WANG Gang, GONG Lun, et al. Research and application of resistance-limiting and energy-dissipating support in Large deformation tunnel[J]. Chinese Journal of Rock Mechanics and Engineering, 2018, 37: 1785–1795.

[14] TAO Zheng-yu. Theory and practice of rock mechanics[M]. Wuhan: Wuhan University Press, 2013: 557–565.

[15] YU Tong-xi, LU Xing-guo. Energy absorption of material and structure[M]. Beijing: Chemical Industry Press, 2006: 14–18.